

PACS numbers: 62.23.Pq, 82.45.Xy

## **Creation and Comparison of Properties of Composites Based on Ceramics Filled with Straight or Helical Carbon Nanotubes for CJP 3D Printing Technology**

Ol. D. Zolotarenko<sup>\*,\*\*</sup>, E. P. Rudakova<sup>\*,\*\*</sup>, An. D. Zolotarenko<sup>\*,\*\*</sup>,  
N. Y. Akhanova<sup>\*\*\*,\*\*\*\*</sup>, M. Ualkhanova<sup>\*\*\*\*</sup>, D. V. Shchur<sup>\*\*</sup>,  
M. T. Gabdullin<sup>\*\*\*</sup>, T. V. Myronenko<sup>\*\*</sup>, A. D. Zolotarenko<sup>\*\*</sup>,  
M. V. Chymbai<sup>\*,\*\*</sup>, and I. V. Zagorulko<sup>\*\*\*\*\*</sup>

<sup>\*</sup>*O. O. Chuiko Institute of Surface Chemistry, NAS of Ukraine,  
17 General Naumov Str.,  
UA-03164 Kyiv, Ukraine*

<sup>\*\*</sup>*I. M. Frantsevich Institute for Problems in Materials Science, NAS of Ukraine,  
3 Omeljan Pritsak Str.,  
UA-03142 Kyiv, Ukraine*

<sup>\*\*\*</sup>*Kazakhstan-British Technical University,  
59 Tole bi Str.,  
050000 Almaty, Republic of Kazakhstan*

<sup>\*\*\*\*</sup>*National Nanotechnology Laboratory, Al-Farabi Kazakh National University,  
71 Al-Farabi Ave.,  
050040 Almaty, Republic of Kazakhstan*

<sup>\*\*\*\*\*</sup>*G. V. Kurdyumov Institute for Metal Physics, NAS of Ukraine,  
36 Academician Vernadsky Blvd.,  
UA-03142 Kyiv, Ukraine*

This paper describes an experiment that made it possible to obtain helical multiwalled carbon nanotubes (HMWCNTs) with a diameter of 30–60 nm by pyrolysis of hydrocarbons and trapping the product with a liquid seal. For the purpose of comparative analysis, the paper also considers the synthesis of straight multiwalled carbon nanotubes (SMWCNTs). Such carbon nanotubes

---

Corresponding author: Oleksandr Dmytrovych Zolotarenko  
E-mail: O.D.Zolotarenko@gmail.com

Citation: Ol. D. Zolotarenko, E. P. Rudakova, An. D. Zolotarenko, N. Y. Akhanova, M. Ualkhanova, D. V. Shchur, M. T. Gabdullin, N. A. Gavrylyuk, T. V. Myronenko, A. D. Zolotarenko, M. V. Chymbai, and I. V. Zagorulko, Creation and Comparison of Properties of Composites Based on Ceramics Filled with Straight or Helical Carbon Nanotubes for CJP 3D Printing Technology, *Metallofiz. Noveishie Tekhnol.*, **45**, No. 2: 199–216 (2023). DOI: 10.15407/mfint.45.02.0199

after preparation can be used in CJP 3D printing technology. All obtained materials are examined using the method of transmission electron microscopy. The paper considers the processes of synthesis of HMWCNTs and SMWCNTs. An assessment of the strength characteristics of 3D products from various composites based on them after discrete 3D printing and sintering is carried out. The conditions for the synthesis of carbon nanostructures by the pyrolytic method are described, methods for preparing synthesis products for their subsequent using in 3D printers of CJP, FDM, SLA, SLS technologies are developed, and the technology for preparing mechanical mixtures for 3D printers of CJP technology is developed. In addition, a technique for creating 3D products from composite materials is considered. The bending strength of 3D printed ceramics reinforced with carbon nanotubes is measured. The dependence of the bending strength of the obtained ceramics on the amount of MWCNTs in the composite is established. The resistance to mechanical destruction of composites (MWCNTs–Al<sub>2</sub>O<sub>3</sub>) obtained using helical and straight MWCNTs is studied. At the same time, it is shown that when using SMWNT, after the integrity of the composite is broken, the parts of the product do not crumble, but remain united even under load.

**Key words:** helical multiwalled carbon nanotubes (HMWCNTs), carbon nanostructures, carbon nanomaterials, carbon nanotubes, single-walled carbon nanotubes, multiwalled carbon nanotubes (MWCNTs), composite, clay, ceramics, Al<sub>2</sub>O<sub>3</sub>, pyrolysis, quartz reactor, Ni, Cu, catalyst, nitrogen (N<sub>2</sub>), toluene (C<sub>7</sub>H<sub>8</sub>), 3D printing, CJP technology, FDM, SLA.

У даній роботі описується експеримент, що дозволив отримати спіралеподібні багатостінні вуглецеві нанорурки (СБВНР) діаметром 30–60 нм шляхом піролізу вуглеводнів та уловлювання продукту рідинним затвором. З метою порівняльного аналізу у роботі розглянуто також синтез прямих багатостінних вуглецевих нанорурок (ПБВНР). Такі вуглецеві нанорурки після виготовлення можна використовувати в технології 3D-друку CJP. Всі отримані матеріали були досліджені за допомогою методу просвічуальної електронної мікроскопії. У роботі розглянуто процеси синтезу СБВНР та ПБВНР. Проведено оцінку характеристик міцності 3D-виробів з різних композитів на їх основі після дискретного 3D-друку та їх спікання. Описано умови синтезу вуглецевих наноструктур піролітичним методом, відпрацьовано методи підготовки продуктів синтезу для подальшого їх використання у 3D-принтерах технології CJP, FDM, SLA, SLS, а також відпрацьовано технологію виготовлення механічних сумішей для 3D-принтерів технології CJP. Крім того, було розглянуто методику створення 3D-виробів із композитних матеріалів. Виміряна міцність на вигин кераміки, створеної методом 3D-друку та армованої вуглецевими нанорурками. Встановлено залежність величини міцності на вигин, отриманої кераміки від кількості БВНР у композиті. Досліджено стійкість до механічного руйнування композитів (БВНР–Al<sub>2</sub>O<sub>3</sub>), отриманих при використанні спіралеподібних та прямих БВНР. У цьому було показано, що з використанням СБВНР після порушення цілісності композиту частини виробу не розсіпаються, а залишаються об'єднаними навіть під навантаженням.

**Ключові слова:** спіральні багатостінні вуглецеві нанорурки (СБВНР), вуглецеві наноструктури, вуглецеві наноматеріали, вуглецеві нанорурки, одностінна вуглецева нанорурка, багатостінні вуглецеві нанорурки, композит, глина, кераміка,  $\text{Al}_2\text{O}_3$ , піроліз, кварцовий реактор, Ni, Cu, каталізатор, азот ( $\text{N}_2$ ), толуол ( $\text{C}_7\text{H}_8$ ), 3D-друк, технологія CJP, FDM, SLA.

(Received October 18, 2022; in final version, November 19, 2022)

## 1. INTRODUCTION

The search for new, more effective methods of synthesizing nanotubes forces scientists to conduct hundreds of experiments. It is difficult to enumerate all the methods [1–7] by which this product is obtained today. However, the issue of large-scale controlled synthesis of carbon nanotubes (CNTs) remains unresolved. Today, there are various per-

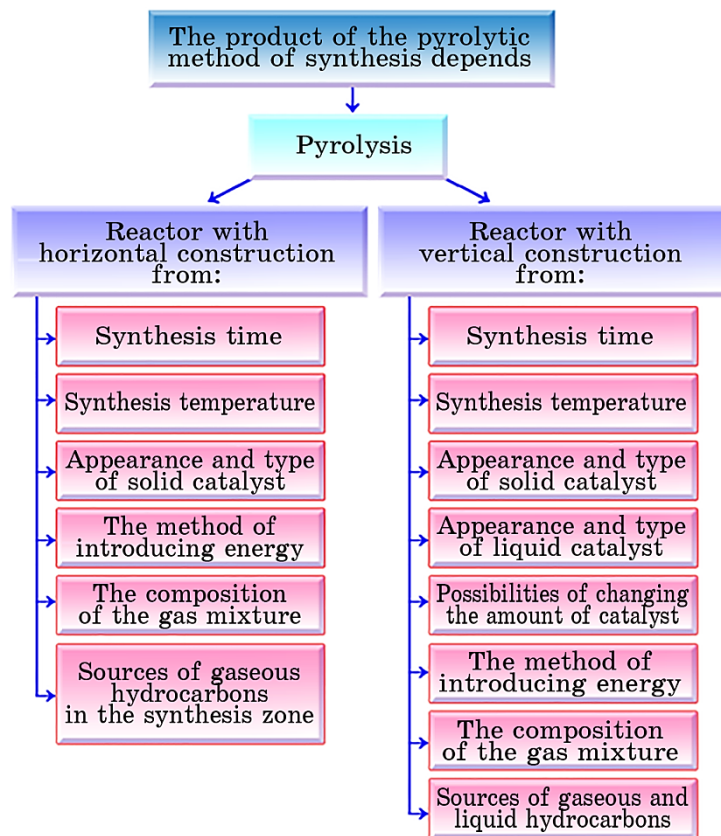


**Fig. 1.** Conditions for the synthesis of products by the pyrolytic method.

spective methods for the synthesis of soluble [8–15] and insoluble [16–20] carbon nanostructures (CNS), which can be used in the creation of new modern materials for 3D printing [21, 22]. Nevertheless, of all the known methods of obtaining CNS, only electric arc evaporation of the anode can guarantee the synthesis of fullerene molecules in large quantities. To date, fullerenes can be used in 3D printing only by SLA technology, which allows changing the properties of the initial material.

Such CNS can be used for hydrogen storage [23–29] and successfully compete with existing materials for hydrogen accumulation [30–55].

Today, it is possible to speak only about a small amount of controlled synthesis of specific CNS. The pyrolytic method makes it possible to easily change the modes of CNS synthesis, to use a gas environment of different chemical composition, and most importantly, to achieve a high percentage of carbon nanotubes of different chemical composition, structure, and morphology in the synthesis products (Fig. 1).

The synthesis of CNS by the pyrolytic method in a horizontal type reactor was carried out by the classical method using gas mixtures (Fig. 2, *a, c*).

The structure and principle of operation of a pyrolytic equipment

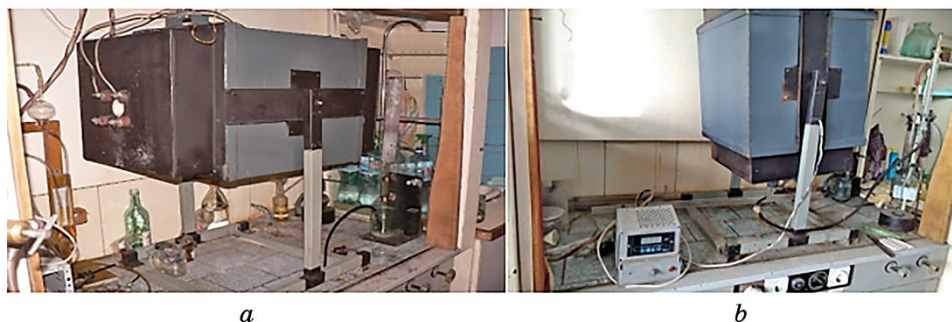
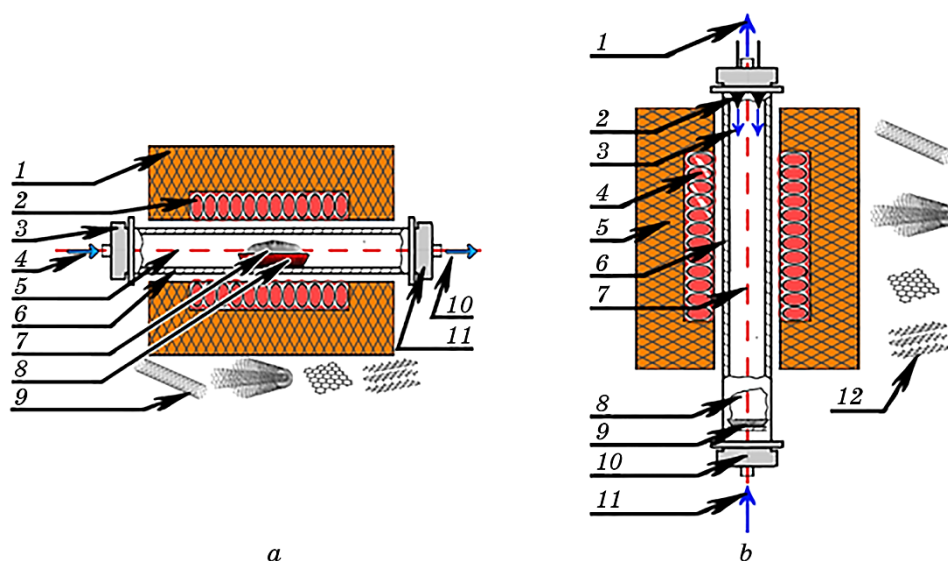


**Fig. 2.** Pyrolytic equipment with a reactor: in a horizontal position (*a*), in a vertical position (*b*), schematic representation of the equipment for the pyrolytic synthesis of CNS when using a horizontal type reactor (1—thermal insulation of the pyrolysis furnace, 2—furnace heaters, 3—reactor inlet flange with thermocouple, 4—directed flow of hydrocarbon gases, 5—axis of the reactor, 6—quartz reactor, 7—catalyst layer, 8—pad, 9—synthesized CNSs, 10—directed flow of gases for utilization, 11—outlet flange of the reactor) (*c*), the principle of operation of the equipment for CNS pyrolytic synthesis when using a vertical type reactor (1—directed flow of hydrocarbon gases, 2—nozzles for supplying solutions, 3—the direction of gravity flows, 4—furnace heaters, 5—thermal insulation of the pyrolysis furnace, 6—quartz reactor, 7—axis of the reactor, 8—carbon nanostructures, 9—platform for collection CNS, 10—reactor flange, 11—supply of hydrocarbon gases, 12—synthesized CNS) (*d*).



Continuation of Fig. 2.

with a special vertical reactor (Fig. 2, *b*, *c*) are similar to a pyrolytic equipment of a horizontal type, but it differs in that both liquid and gaseous hydrocarbons (or their mixtures) can be used as carbon sources in the synthesis zone.

## 2. EXPERIMENTAL PART AND RESULTS

### 2.1. The Synthesis of Helical Multiwalled Carbon Nanotubes

The synthesis of helical multiwalled carbon nanotubes (HMWCNTs) was carried out in a vertical reactor, where acetylene and toluene vapor were used as a carbon source. The process was carried out in a quartz reactor on nickel–copper (Ni–Cu) catalysts in a stream of nitrogen.

Carbon nanotubes and fibres were synthesized from both acetylene and toluene vapours in the temperature range of 800–1500 K. During the synthesis of MWCNT from toluene vapour at 1155 K, a dark brown condensate was formed in the cooler part of the reactor. When acetylene is passed through the reactor, this liquid reacts with the gas phase, turning into smoke. The smoke is captured by a liquid shutter.

Using the method of electron microscopy of the synthesis products (Fig. 3), it was shown that under these experimental conditions, the helical nanofibers with a diameter of 15–60 nm with a coil pitch of 100 nm are formed, and the average diameter of the spiral itself is 70 nm (Fig. 3, *a*). Spirals have different configurations, they can be

come straight (Fig. 3, *c, d*), intertwine (Fig. 3, *c, e*) or form y-shaped shapes (Fig. 3, *c, d, e*).

Helical synthesis products were analysed by Raman spectroscopy, which confirms the presence of multilayered carbon tubular formation

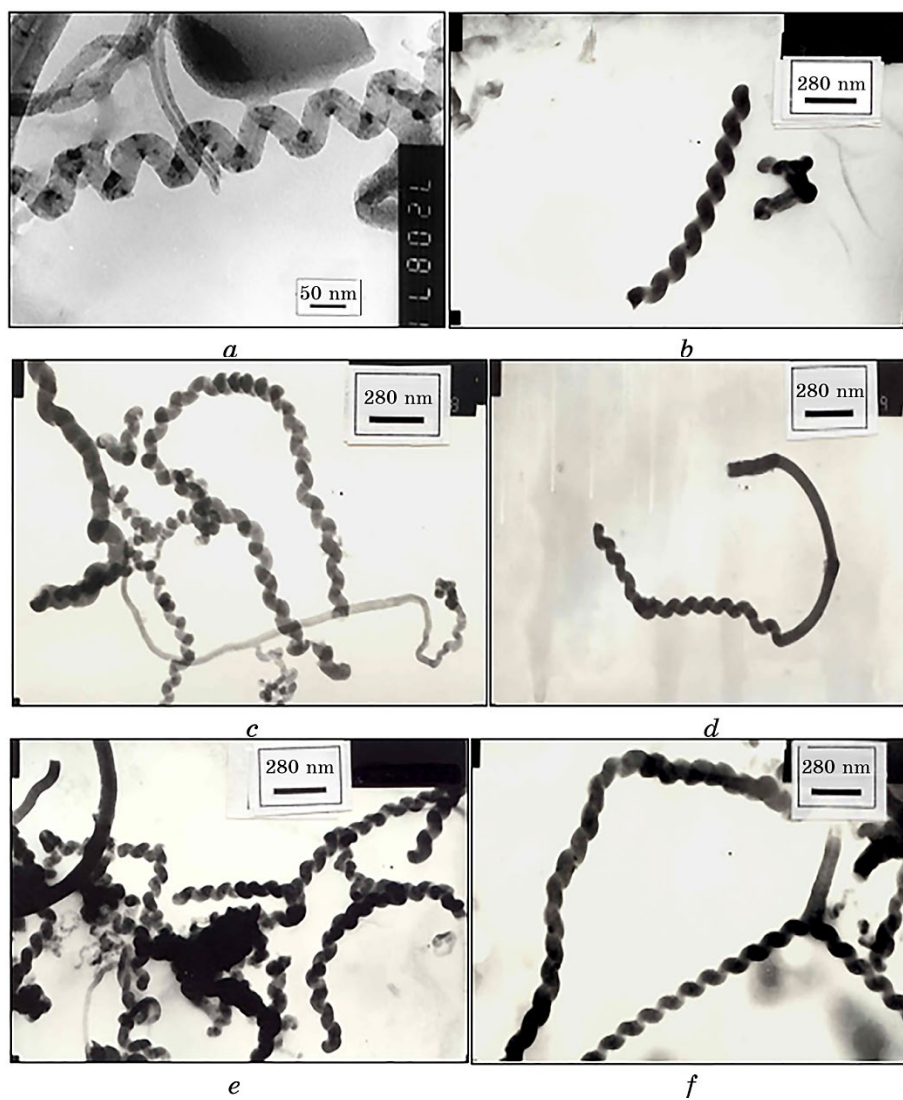


**Fig. 3.** Electron transmission microscopy of the product of synthesis of helical multiwalled carbon nanotubes (HMWCNTs) in a vertical pyrolytic reactor. Changes in HMWCNT: structure of HMWCNT (*a, b*), HMWCNT are intertwined (*c*), HMWCNTs transitioning into straight CNTs (*d*), HMWCNTs form y-type shapes (*e*).



**TABLE 1.** Results of thermal analysis of helical multiwalled carbon nanotubes (HMWCNTs).

No.	Material	Temperature interval of thermal interaction, K	DTG		DTA	
			$T_{1\max}$ , K	$T_{2\max}$ , K	$T_{1\max}$ , K	$T_{2\max}$ , K
1	Acetylene pyrolysis product on Ni–Cu catalyst at 1500 K	669–973	859	–	863	–
2	Acetylene pyrolysis product on Ni–Cu catalyst at 800 K	673–803	718	738	718	753

in the synthesis product, *i.e.*, MWCNT (Fig. 4, *a*).

Thermal analysis with air oxygen of the pyrolysis products of acetylene on a Ni–Cu catalyst, obtained at a synthesis temperature of 1500 K (Fig. 4, *b*, curve 1), Table 1, item 1), showed that CNS were oxidized in a wide temperature range (668–973 K), but the maximum speed of the process was observed at the temperature values  $T_{\max} = 859$  K (Table 1, items 1, 2).

Probably, during the pyrolysis of acetylene, in addition to carbon nanotubes, amorphous carbon of various modifications is formed, which has different heat resistance (Fig. 4, *b*).

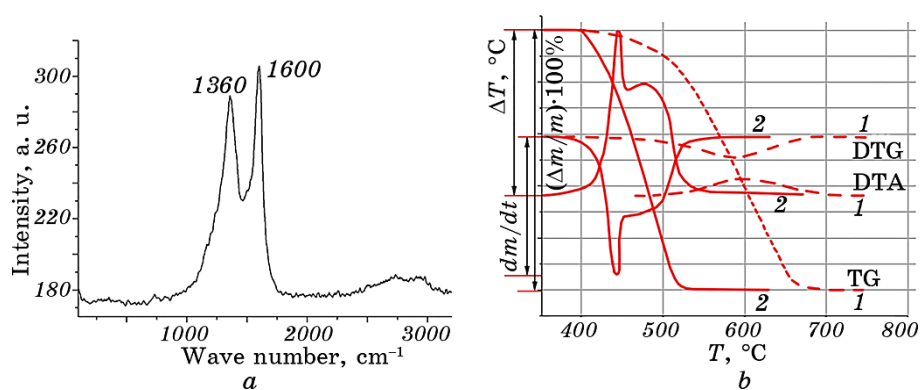


**Fig. 4.** Analysis of products of pyrolytic synthesis of HMWCNTs: Raman spectrum of HMWCNTs, which confirms the presence of nanotubes in the synthesis product (*a*), thermogram of the pyrolysis product of acetylene on Ni–Cu catalyst: 1—at 1500 K (dashed line), 2—at 800 K (solid line) (*b*).

## 2.2. The Synthesis of Straight Multiwalled Carbon Nanotubes

The synthesis of straight multiwalled carbon nanotubes was carried out in a horizontal type reactor (Fig. 2, *a*, *c*), where gaseous hydrocarbons and their mixtures at atmospheric pressure were used as a carbon source.

The catalyst (iron powder) on a ceramic substrate was installed in the middle of the quartz reactor. Before the synthesis process, the reactor was filled with an inert gas (argon) and heated from 900 K to 1500 K with its weak flow. At a temperature of 1200 K, a mixture of methane gas ( $\text{CH}_4$ ) and hydrogen ( $\text{H}_2$ ) was fed in a ratio of 2:1. When the synthesis was stopped, the horizontal reactors of the CNS were cooled in a stream of hydrogen.

The method of transmission electron microscopy (Fig. 5) confirmed a high yield of the product with the content of formed straight and slightly curved MWCNTs, where the diameter of the nanofibers reached from 5 nm to 60 nm. Raman spectroscopy of the synthesis products also indicates the presence of MWCNTs in the pyrolytic synthesis product (Fig. 6, *a*).

Thermal analysis of unrefined straight multilayer carbon nanotubes

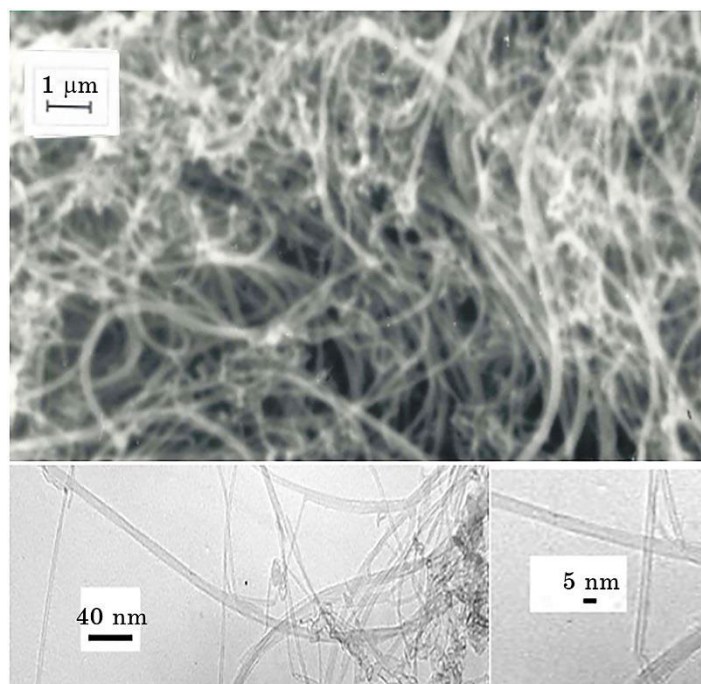


**Fig. 5.** Electron transmission microscopy of the synthesis product of straight multiwalled carbon nanotubes (SMWCNTs) in a horizontal pyrolytic reactor.



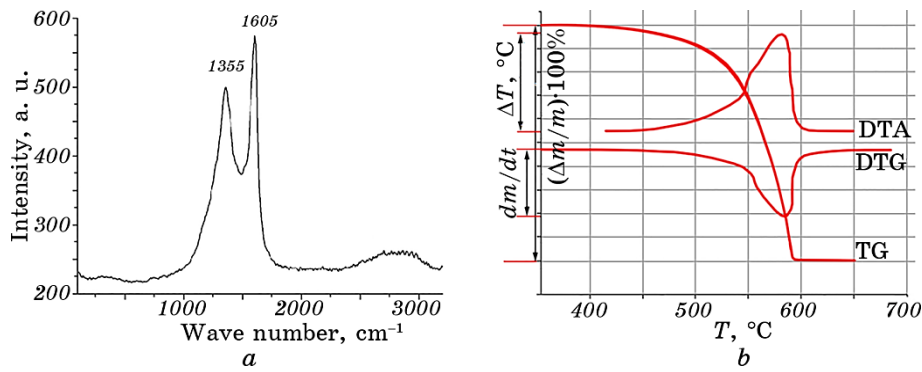


**Fig. 6.** Analysis of synthesis products: Raman spectrum of straight MWCNTs, which confirms the presence of nanotubes in the synthesis product (*a*), thermogram of unrefined straight MWCNTs obtained by the pyrolysis method at 1200 K (*b*).

**TABLE 2.** Results of thermal analysis of straight multiwalled carbon nanotubes (SMWCNTs).

No.	Material	Temperature interval of thermal interaction, K	DTG	DTA
			$T_{\max}$ , K	$T_{\max}$ , K
1	Unrefined straight MWCNTs obtained by pyrolysis at 1200 K	673–883	859	858

obtained by pyrolysis at 1200 K showed that they were oxidized in the temperature range 673–883 K. This process corresponds to the exhibition of two sharp peaks ( $T_{\max} = 859$  K and 858 K) on the DTG and DTA curves (Fig. 6, *b*, Table 2, item 1). Such indicators may prove good homogeneity of the sample obtained under the specified conditions.

### 2.3. Creation of a Mechanical Mixture of Metal Oxide–MWCNT (MWCNT– $\text{Al}_2\text{O}_3$ ) for 3D Printers of CJP Technology

After technological processing, mesoscopic MWCNT systems can be used to manufacturing of mechanical mixtures for CJP (MWCNT–ceramic) 3D printers or to create consumable composite materials for FDM, SLS (MWCNT–solid polymer) and SLA (MWCNT–liquid polymer) 3D printing technologies.

Mechanical mixtures for CJP technology 3D printers are prepared by thoroughly mixing grinded MWCNTs and sieved ceramics (in our case,  $\text{Al}_2\text{O}_3$ ) for 3 hours. This procedure contributes to obtaining a homogeneous mechanical mixture, where the MWCNTs are uniformly

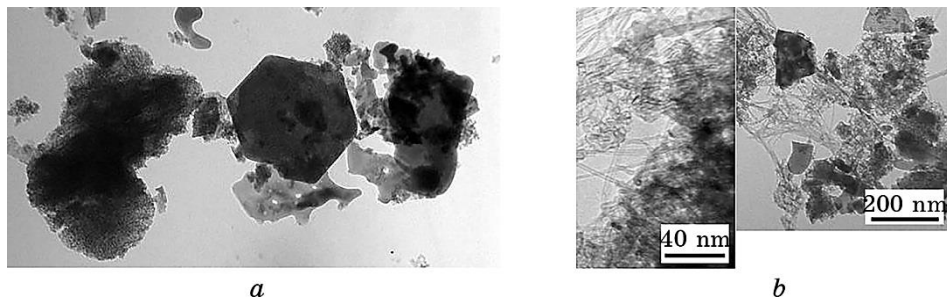


**Fig. 7.** Photomicrograph of the original powder of aluminium oxide ( $\text{Al}_2\text{O}_3$ ) (a) and composite in which ceramics are reinforced with CNT (b).

distributed in the volume. This is the main rule for creating a high-quality 3D product from the considered composite.

Both aluminium oxide ( $\text{Al}_2\text{O}_3$ ) in its initial state (Fig. 7, a) and a composite based on this ceramic reinforced with straight MWCNTs (Fig. 7, b) were examined by scanning electron microscopy. At the same time, a uniform distribution of MWCNT was observed in the volume of

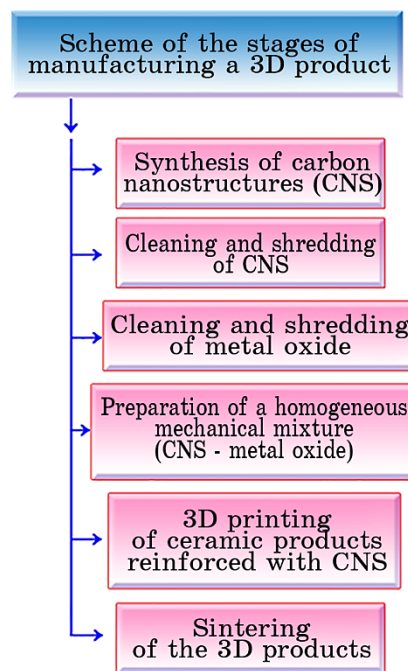


**Fig. 8.** Scheme of the stages of manufacturing a 3D composite product (CNS–ceramics).

the mechanical mixture.

#### 2.4. 3D Products (CJP) from Composite Materials (MWCNT–Al<sub>2</sub>O<sub>3</sub>)

The procedure for manufacturing 3D products for CJP technology from a composite (CNS–metal oxide) can be presented in the form of a diagram (Fig. 8).

CJP (ColorJet Printing) or 3DP (3D Printing) technology is an additive technology of injection manufacturing of three-dimensional objects by the method of discrete layer-by-layer printing (Fig. 9), where the consumables have a loose powder form (ceramics, plaster, plastic, CNS, *etc.*). Each layer of printing is impregnated with an adhesive.

The 3D printing process is carried out at a temperature of 300–

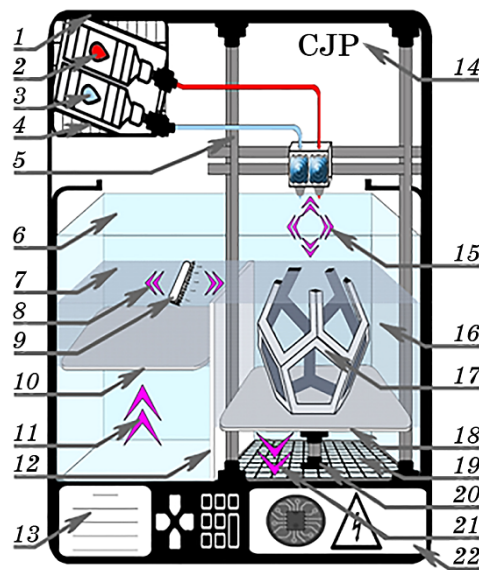


**Fig. 9.** Scheme of the operation principle of CJP 3D printing technology: 1—CJP 3D printer body, 2—consumables, 3—consumable material of binder, 4—hermetic compartment for consumables, 5—build platform and print head guides, 6—working compartment of the 3D printer, 7—camera with 3D printer consumables (ceramics with CNS), 8—the direction of the layering brush, 9—layering brush for construction, 10—platform for consumables supplying, 11—the direction of platform movement, 12—blind partition of the working compartment, 13—3D printer control panel, 14—3D printer print type, 15—the direction of movement of the print head of the 3D printer, 16—camera for 3D products building, 17—3D product from CNS, 18—a platform for 3D products building, 19—ports for cleaning the construction chamber, 20—construction platform guide, 21—the direction of platform movement, 22—the electronic part of the 3D printer.



**Fig. 10.** Composite 3D sample of metal oxide reinforced with MWCNT (CJP technology).

315 K. Thus, the low cost of consumables combined with an operating temperature close to room temperature favourably distinguishes CJP printing technology from other in terms of economy and profitability. However, the 3D printed product is not the final product and requires post-moulding processing to give the material the required physico-chemical and mechanical properties.

After that, sintering (annealing) of the 3D product was carried out in a high-temperature vacuum electric furnace (Fig. 10) under conditions of gradual heating to 2050 K, followed by holding at the maximum temperature for 2 hours.

**TABLE 3.** Literary data on the strength characteristics of various ceramics in comparison with the obtained composite (MWCNT–Al<sub>2</sub>O<sub>3</sub>).

	Bending strength limit, MPa	Crack resistance, MPa·m <sup>0.5</sup>	Vickers hardness, GPa	Density, g/cm <sup>3</sup>	Young's modulus, GPa	Reference
Zirconium dioxide stabilized by yttrium oxide (ZrO <sub>2</sub> (Y <sub>2</sub> O <sub>3</sub> ))	750–1050	8.0–10.0	12.0–13.0	6.00–6.05	200–210	[56]
MWCNT–Al <sub>2</sub> O <sub>3</sub> (1:1) composite	620	7.0	19.0	–	–	–
Silicon carbide (SiC)	350–450	3.0–4.0	23.0–28.0	3.12–3.17	390–420	[57]
Aluminium oxide (Al <sub>2</sub> O <sub>3</sub> )	300–350	3.0–3.5	19.0–21.0	3.80–3.90	370–380	[57, 58]
Spinel (MgAl <sub>2</sub> O <sub>4</sub> )	250–350	2.0	20.0	3.57–3.72	230	[58]

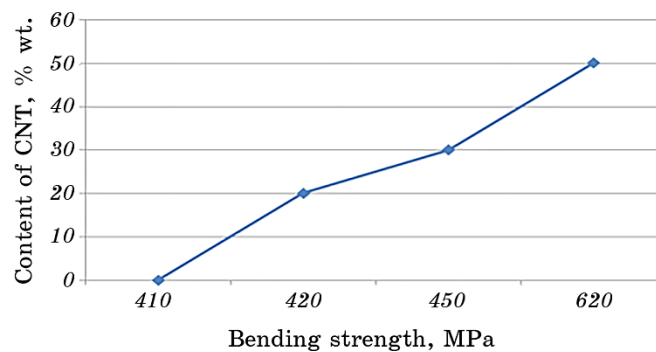
**TABLE 4.** Strength indicators for the MWCNT–Al<sub>2</sub>O<sub>3</sub> composite after its 3D printing and sintering.

Content of MWCNT in Al <sub>2</sub> O <sub>3</sub> , % wt.	Bending strength, MPa	Porosity, %	Microhardness, GPa	Crack resistance, MPa·m <sup>0.5</sup>
0	410	7.0	20.0	9.0
20	420	3.0	18.0	5.0
30	450	5.0	18.0	5.5
50	620	~ 1.0	19.0	7.0

Thus, the following conditions were selected for the sintering of a 3D composite product (MWCNT–ceramics): rarefied environment— $10^{-3}$  mm Hg, the maximum sintering temperature is from 2000 K to 2100 K.

The results of the analysis of the strength characteristics of various ceramics in comparison with the composite MWCNT–Al<sub>2</sub>O<sub>3</sub> (1:1) after its 3D printing are shown in Table 3. The strength values for the composite (MWCNT–Al<sub>2</sub>O<sub>3</sub>) with different content of MWCNT (0–50% wt.) after 3D printing were also obtained. The results of the research (Table 4) showed a directly proportional increase in bending strength from the amount of MWCNT in the composite sample after its 3D printing (Fig. 11).

As a result of the experiments, an increase in the strength to mechanical destruction of the composite (MWCNT–Al<sub>2</sub>O<sub>3</sub>) was noted when using spiral-shaped MWCNTs compared to straight MWCNTs. This means that the 3D printed sample, after quenching, the composite filled with HMWCNTs does not fall apart when fractured, unlike the composite (SMWCNTs–Al<sub>2</sub>O<sub>3</sub>), which contains straight multiwalled

**Fig. 11.** Dependence of the bending strength value on the number of straight MWCNTs in the composite sample after 3D printing and sintering.

**TABLE 5.** Comparison of strength indicators for composites reinforced with helical or straight MWCNT.

Content of MWCNT in Al <sub>2</sub> O <sub>3</sub> , % wt.	Bending strength of the composite with straight MWCNTs, MPa	Bending strength of the composite with helical MWCNTs, MPa
0	410	410
20	420	415
30	450	445
50	620	610

carbon nanotubes. Perhaps, this is due to the structure of the MWCNT, which is a system of CNT cylinders inserted into each other. When the outer cylinders (shells) of straight MWCNTs break, the inner MWCNTs can be removed by pushing them relative to each other. At the same time, HMWCNT does not have a similar effect due to its spiral structure.

### 3. CONCLUSIONS

1. A method for obtaining conglomerates of helical multiwalled carbon nanotubes (CNTs) with a diameter of 15–60 nm is proposed.
2. A diagram of the conditions for the CNS synthesis by the pyrolytic method was created.
3. A new equipment for the pyrolytic synthesis of CNS was developed and created.
4. A diagram of the technological stages of manufacturing a 3D composite product (CNS–ceramics) has been created.
5. The technology for the synthesis of multiwalled carbon nanotubes (MWCNTs) of different configurations (straight and helical) for 3D printing of CJP technology has been developed.
6. The conditions for printing with a mechanical mixture of MWCNT–Al<sub>2</sub>O<sub>3</sub> for a CJP technology 3D printer have been established.
7. The process of creating of mechanical mixtures (MWCNT–metal oxide) for 3D printers of CJP technology is considered.
8. It has been established that the main rule for creating a high-quality 3D product in the CJP technology from a composite reinforced with MWCNT is the creation of a high-quality homogeneous mechanical mixture prepared by thoroughly mixing crushed MWCNT conglomerates and processed metal oxide—the supporting ceramic matrix, where the MWCNTs are evenly distributed in the mixture. In the mechanical mixture, the size of aluminium oxide is  $\geq 100$  nm ( $\geq 0.1$   $\mu$ m), and the



MWCNTs have a diameter of  $\leq 60$  nm and a length of  $\geq 925$  nm.

9. A directly proportional dependence of the increase in bending strength on the content of MWCNT in a 3D composite product (MWCNT–metal oxide) after its 3D printing and sintering was established.

10. A comparative analysis of the strength of 3D products made of composites based on straight multiwalled carbon nanotubes (SMWCNT) and helical multiwalled carbon nanotubes (HMWCNT) was carried out.

11. It was established that composites based on straight MWCNTs have greater strength than composites based on HMWCNTs.

## REFERENCES

1. V. A. Lavrenko, I. A. Podchernyaeva, D. V. Shchur, An. D. Zolotarenko, and Al. D. Zolotarenko, *Powder Metallurgy and Metal Ceramics*, **56**: 504 (2018).
2. Ol. D. Zolotarenko, M. N. Ualkhanova, E. P. Rudakova, N. Y. Akhanova, An. D. Zolotarenko, D. V. Shchur, M. T. Gabdullin, N. A. Gavrylyuk, A. D. Zolotarenko, M. V. Chymbai, I. V. Zagorulko, and O. O. Havryliuk, *Chemistry, Phys. Tech. Surf.*, **13**, No. 2: 209 (2022).
3. Z. A. Matysina, Ol. D. Zolotarenko, M. Ualkhanova, O. P. Rudakova, N. Y. Akhanova, An. D. Zolotarenko, D. V. Shchur, M. T. Gabdullin, N. A. Gavrylyuk, O. D. Zolotarenko, M. V. Chymbai, and I. V. Zagorulko, *Prog. Phys. Met.*, **23**, No. 3: 528 (2022).
4. A. D. Zolotarenko, A. D. Zolotarenko, E. P. Rudakova, S. Y. Zaginaichenko, A. G. Dubovoy, D. V. Schur, and Y. A. Tarasenko, *Carbon Nanomaterials in Clean Energy Hydrogen Systems-II* (Dordrecht: Springer: 2007), p. 137.
5. D. V. Schur, A. G. Dubovoy, S. Yu. Zaginaichenko, V. M. Adejev, A. V. Kotko, V. A. Bogolepov, A. F. Savenko, A. D. Zolotarenko, S. A. Firstov and V. V. Skorokhod, *NATO Security through Science Series A: Chemistry and Biology*: 199 (2007).
6. S. Yu. Zaginaichenko, D. V. Schur, and Z. A. Matysina, *Carbon*, **41**, Iss. 7: 1349 (2003).
7. V. A. Lavrenko, D. V. Shchur, A. D. Zolotarenko, and A. D. Zolotarenko, *Powder Metallurgy and Metal Ceramics*, **57**, No. 9: 596 (2019).
8. V. M. Gun'ko, V. V. Turov, D. V. Schur, V. I. Zarko, G. P. Prykhod'ko, T. V. Krupska, A. P. Golovan, J. Skubiszewska-Zięba, B. Charnas, and M. T. Kartel, *Chem. Phys.*, **459**: 172 (2015).
9. M. M. Nishchenko, S. P. Likhtorovich, D. V. Schur, A. G. Dubovoy, and T. A. Rashevskaya, *Carbon*, **41**, No. 7: 1381 (2003).
10. D. V. Schur, S. Yu. Zaginaichenko, E. A. Lysenko, T. N. Golovchenko, and N. F. Javadov, *Carbon Nanomaterials in Clean Energy Hydrogen Systems*, (Dordrecht: Springer: 2008), p. 53.
11. D. V. Schur, S. Yu. Zaginaichenko, A. D. Zolotarenko, and T. N. Veziroglu, *Carbon Nanomaterials in Clean Energy Hydrogen Systems*, (Dordrecht: Springer: 2008), p. 85.
12. O. D. Zolotarenko, O. P. Rudakova, M. T. Kartel, H. O. Kaleniuk,

- A. D. Zolotarenko, D. V. Schur, and Y. O. Tarasenko, *Surface*, **12**, No. 27: 263 (2020) (in Ukrainian).
13. N. E. Ahanova, D. V. Schur, N. A. Gavriluk, M. T. Gabdullin, N. S. Anikina, An. D. Zolotarenko, O. Ya. Krivushhenko, Al. D. Zolotarenko, B. M. Gorelov, E. Erlanuli, and D. G. Batrishev, *Chemistry, Physics and Technology of Surface*, **11**, No. 3: 429 (2020) (in Ukrainian).
14. Z. A. Matysina, Ol. D. Zolotarenko, O. P. Rudakova, N. Y. Akhanova, A. P. Pomytkin, An. D. Zolotarenko, D. V. Shchur, M. T. Gabdullin, M. Ualkhanova, N. A. Gavrylyuk, A. D. Zolotarenko, M. V. Chymbai, and I. V. Zagorulko, *Prog. Phys. Met.*, **23**, No. 3: 510 (2022).
15. N. Ye. Akhanova, D. V. Shchur, A. P. Pomytkin, Al. D. Zolotarenko, An. D. Zolotarenko, N. A. Gavrylyuk, M. Ualkhanova, W. Bo, and D. Ang, *J. Nanosci. Nanotechnol.*, **21**: 2435 (2021).
16. O. D. Zolotarenko, E. P. Rudakova, A. D. Zolotarenko, N. Y. Akhanova, M. N. Ualkhanova, D. V. Shchur, M. T. Gabdullin, N. A. Gavrylyuk, T. V. Myronenko, A. D. Zolotarenko, M. V. Chymbai, I. V. Zagorulko, Yu. O. Tarasenko, and O. O. Havryliuk, *Chemistry, Physics and Technology of Surface*, **13**, No. 3: 259 (2022) (in Ukrainian).
17. D. V. Schur, A. D. Zolotarenko, A. D. Zolotarenko, O. P. Zolotarenko, M. V. Chimbai, N. Y. Akhanova, M. Sultangazina, and E. P. Zolotarenko, *Phys. Sci. Tech.*, **6**, No. 1–2: 46 (2019).
18. M. Baibarac, I. Baltog, S. Frunza, A. Magrez, D. Schur, and S. Zaginaichenko, *Diamond Relat. Mater.*, **32**: 72 (2013).
19. A. D. Zolotarenko, A. D. Zolotarenko, V. A. Lavrenko, S. Y. Zaginaichenko, N. A. Shvachko, O. V. Milto, and Y. A. Tarasenko, *Carbon Nanomaterials in Clean Energy Hydrogen Systems-II*: 127 (2011).
20. N. Akhanova, S. Orazbayev, M. Ualkhanova, A. Y. Perekos, A. G. Dubovoy, D. V. Schur, Al. D. Zolotarenko, An. D. Zolotarenko, N. A. Gavrylyuk, M. T. Gabdullin, and T. S. Ramazanov, *J. Nanosci. Nanotech. Applications*, **3**, No. 3: 1 (2019).
21. Ol. D. Zolotarenko, O. P. Rudakova, N. E. Ahanova, An. D. Zolotarenko, D. V. Schur, M. T. Gabdullin, M. Ualhanova, N. A. Gavriluk, M. V. Chimbaj, Yu. O. Tarasenko, I. V. Zagorulko, and O. D. Zolotarenko, *Metallofiz. Noveishie Tekhnol.*, **43**, No. 10: 1417 (2021) (in Ukrainian).
22. Ol. D. Zolotarenko, E. P. Rudakova, N. Y. Akhanova, An. D. Zolotarenko, D. V. Shchur, M. T. Gabdullin, M. Ualkhanova, M. Sultangazina, N. A. Gavrylyuk, M. V. Chymbai, A. D. Zolotarenko, I. V. Zagorulko, and Yu. O. Tarasenko, *Metallofiz. Noveishie Tekhnol.*, **44**, No. 3: 343 (2022) (in Ukrainian).
23. D. V. Schur, S. Y. Zaginaichenko, A. F. Savenko, V. A. Bogolepov, and N. S. Anikina, *Int. J. Hydrogen Energy*, **36**, No. 1: 1143 (2011).
24. A. F. Savenko, V. A. Bogolepov, K. A. Meleshevich, S. Yu. Zaginaichenko, D. V. Schur, M. V. Lototsky, V. K. Pishuk, L. O. Teslenko, and V. V. Skorokhod, *Hydrogen Materials Science and Chemistry of Carbon Nanomaterials*: 365 (2007).
25. D. V. Schur, S. Zaginaichenko, and T. N. Veziroglu, *Int. J. Hydrogen Energy*, **33**, Iss. 13: 3330 (2008).
26. D. V. Schur, M. T. Gabdullin, S. Yu. Zaginaichenko, T. N. Veziroglu, M. V. Lototsky, V. A. Bogolepov, and A. F. Savenko, *Int. J. Hydrogen Energy*,

- [41, Iss. 1: 401\(2016\).](#)
27. D. V. Schur, S. Yu. Zaginaichenko, and T. N. Veziroglu, *Int. J. Hydrogen Energy*, **40**, Iss. 6: 2742 (2015).
28. Z. A. Matysina, S. Yu. Zaginaichenko, D. V. Shchur, A. Veziroglu, T. N. Veziroglu, M. T. Gabdullin, N. F. Javadov, An. D. Zolotareno and Al. D. Zolotareno, *Gidrogen v Kristallah* [Hydrogen in Crystals] (Kyiv: Publishing House 'KIM': 2017) (in Russian).
29. D. V. Schur, S. Yu. Zaginaichenko, A. F. Savenko, V. A. Bogolepov, N. S. Anikina, A. D. Zolotareno, Z. A. Matysina, T. N. Veziroglu and N. E. Skryabina, *Carbon Nanomaterials in Clean Energy Hydrogen Systems-II*: **87** (2011).
30. Z. A. Matysina, An. D. Zolotareno, Al. D. Zolotareno, N. A. Gavrylyuk, A. Veziroglu, T. N. Veziroglu, A. P. Pomytkin, D. V. Schur, and M. T. Gabdullin, *Features of the Interaction of Hydrogen with Metals, Alloys and Compounds. Hydrogen Atoms in Crystalline Solids* (Kyiv: 'KIM' Publishing House: 2022).
31. D. V. Schur, M. T. Gabdullin, V. A. Bogolepov, A. Veziroglu, S. Yu. Zaginaichenko, A. F. Savenko, and K. A. Meleshevich, *Int. J. Hydrogen Energy*, **41**, Iss. 3: 1811 (2016).
32. Z. A. Matysina and D. V. Shchur, *Russ. Phys. J.*, **44**: 1237 (2001).
33. V. I. Trefilov, D. V. Schur, V. K. Pishuk, S. Yu. Zaginaichenko, A. V. Choba, and N. R. Nagornaya, *Renewable Energy*, **16**, Iss. 1–4: 757 (1999).
34. A. D. Zolotareno, A. D. Zolotareno, A. Veziroglu, T. N. Veziroglu, N. A. Shvachko, A. P. Pomytkin, N. A. Gavrylyuk, D. V. Schur, T. S. Ramazanov, and M. T. Gabdullin, *Int. J. Hydrogen Energy*, **47**, Iss. 11: 7281 (2022).
35. Ol. D. Zolotareno, O. P. Rudakova, An. D. Zolotareno, D. V. Shchur, N. A. Gavrylyuk, N. T. Kartel, O. D. Zolotareno, and V. A. Mashira, *Recent Contributions to Physics*, **81**, No. 2: 68 (2022) (in Russian).
36. Z. A. Matysina, O. S. Pogorelova, S. Yu. Zaginaichenko, and D. V. Schur, *J. Phys. Chem. Solids*, **56**, No. 1: 9 (1995).
37. Z. A. Matysina, S. Yu. Zaginaichenko, and D. V. Schur, *Int. J. Hydrogen Energy*, **21**, Is. 11–12: 1085 (1996).
38. D. V. Schur, S. Yu. Zaginaichenko, Z. A. Matysina, I. Smityukh, and V. K. Pishuk, *J. Alloys Comd.*, **330–332**: 70 (2002).
39. Yu. M. Lytvynenko and D. V. Schur, *Renewable Energy*, **16**, No. 1: 753 (1999).
40. D. V. Schur, A. A. Lyashenko, V. M. Adejev, V. B. Voitovich, and S. Yu. Zaginaichenko, *Int. J. Hydrogen Energy*, **20**, Iss. 5: 405 (1995).
41. D. V. Schur, V. A. Lavrenko, V. M. Adejev, and I. E. Kirjakova, *Int. J. Hydrogen Energy*, **19**, Iss. 3: 265 (1994).
42. Z. A. Matysina, S. Yu. Zaginaichenko, D. V. Shchur, and M. T. Gabdullin, *Russ. Phys. J.*, **59**, No. 2: 177 (2016).
43. S. Yu. Zaginaichenko, Z. A. Matysina, D. V. Schur, L. O. Teslenko, and A. Veziroglu, *Int. J. Hydrogen Energy*, **36**, Iss. 1: 1152 (2011).
44. S. Yu. Zaginaichenko, D. A. Zaritskii, D. V. Schur, Z. A. Matysina, T. N. Veziroglu, M. V. Chymbai, and L. I. Kopylova, *Int. J. Hydrogen Energy*, **40**, Iss. 24: 7644 (2015).
45. Z. A. Matysina, S. Yu. Zaginaichenko, and D. V. Shchur, *Fiz. Met. Metalloved.*, **114**, No. 4: 308 (2013).

46. Z. A. Matysina, N. A. Gavrylyuk, M. T. Kartel, A. Veziroglu, T. N. Veziroglu, A. P. Pomytkin, D. V. Schur, T. S. Ramazanov, M. T. Gabdullin, An. D. Zolotarenko, Al. D. Zolotarenko, and N. A. Shvachko, *Int. J. Hydrogen Energy*, **46**, Iss. 50: 25520 (2021).
47. D. V. Shchur, S. Yu. Zaginaichenko, A. Veziroglu, T. N. Veziroglu, N. A. Gavrylyuk, A. D. Zolotarenko, M. T. Gabdullin, T. S. Ramazanov, Al. D. Zolotarenko, and An. D. Zolotarenko, *Russ. Phys. J.*, **64**: 89 (2021).
48. S. Yu. Zaginaichenko, Z. A. Matysina, D. V. Schur, and A. D. Zolotarenko, *Int. J. Hydrogen Energy*, **37**, Iss. 9: 7565 (2012).
49. S. A. Tikhotskii, I. V. Fokin, and D. V. Schur, *Izvestiya, Physics of the Solid Earth*, **47**, No. 4: 327 (2011).
50. A. D. Zolotarenko, A. D. Zolotarenko, A. Veziroglu, T. N. Veziroglu, N. A. Shvachko, A. P. Pomytkin, D. V. Schur, N. A. Gavrylyuk, T. S. Ramazanov, N. Y. Akhanova, and M. T. Gabdullin, *Int. J. Hydrogen Energy*, **47**, Iss. 11: 7310 (2022).
51. Z. A. Matysina, S. Yu. Zaginaichenko, D. V. Schur, T. N. Veziroglu, A. Veziroglu, M. T. Gabdullin, Al. D. Zolotarenko, and An. D. Zolotarenko, *Int. J. Hydrogen Energy*, **43**, Iss. 33: 16092 (2018).
52. Z. A. Matysina, S. Yu. Zaginaichenko, D. V. Schur, A. D. Zolotarenko, A. D. Zolotarenko, M. T. Gabdulin, L. I. Kopylova, and T. I. Shaposhnikova, *Russ. Phys. J.*, **61**: 2244 (2019).
53. D. V. Schur, A. Veziroglu, S. Yu. Zaginaychenko, Z. A. Matysina, T. N. Veziroglu, M. T. Gabdullin, T. S. Ramazanov, A. D. Zolotarenko, and A. D. Zolotarenko, *Int. J. Hydrogen Energy*, **44**, Iss. 45: 24810 (2019).
54. Z. A. Matysina, S. Yu. Zaginaichenko, D. V. Schur, Al. D. Zolotarenko, An. D. Zolotarenko, and M. T. Gabdullin, *Russ. Phys. J.*, **61**: 253 (2018).
55. An. D. Zolotarenko, Al. D. Zolotarenko, A. Veziroglu, T. N. Veziroglu, N. A. Shvachko, A. P. Pomytkin, N. A. Gavrylyuk, D. V. Schur, T. S. Ramazanov, and M. T. Gabdullin, *Int. J. Hydrogen Energy*, **44**, Iss. 11: 7281 (2021).
56. S. E. Porozova, L. D. Sirotenko, V. O. Shokov, and A. A. Gurov, *Refract. Ind. Ceram.*, **57**: 321 (2016).
57. K. Ando, B.-S. Kim, M.-C. Chu, S. Saitou, and S. Sato, *Key Engineering Materials*, **247**: 175 (2003).
58. D. Mittal, J. Hostaša, L. Silvestroni, L. Esposito, A. Mohan, R. Kumar, and S. K. Sharma, *J. European Ceramic Society*, **42**, Iss. 14: 6303 (2022).